







# Scaling of average power in sub-MW peak power Yb-doped tapered fiber picosecond pulse amplifiers

KONSTANTIN BOBKOV,<sup>1</sup> ANDREY LEVCHENKO,<sup>1</sup> TATIANA KASHAYKINA,<sup>1</sup>  SVETLANA ALESHKINA,<sup>1</sup>  MIKHAIL BUBNOV,<sup>1</sup> DENIS LIPATOV,<sup>2</sup> ALEKSANDR LAPTEV,<sup>2</sup> ALEXEY GURYANOV,<sup>2</sup> YANN LEVENTOUX,<sup>3</sup> GEOFFROY GRANGER,<sup>3</sup> VINCENT COUDERC,<sup>3</sup>  SÉBASTIEN FÉVRIER,<sup>3</sup>  AND MIKHAIL LIKHACHEV<sup>1,\*</sup>

<sup>1</sup>Prokhorov General Physics Institute of the Russian Academy of Sciences, Dianov Fiber Optics Research Center, 38 Vavilov Street, Moscow 119333, Russia

<sup>2</sup>Institute of Chemistry of High Purity Substances of the Russian Academy of Science, Nizhny Novgorod 603950, Russia

<sup>3</sup>Université de Limoges, XLIM, UMR CNRS 7252, 123 Av. A. Thomas, Limoges 87000, France

\*likhachev@fo.gpi.ru

**Abstract:** Prospects for average power scaling of sub-MW output peak power picosecond fiber lasers by utilization of a Yb-doped tapered fiber at the final amplification stage were studied. In this paper, it was shown experimentally that a tapered fiber allows the achievement of an average power level of 150 W (limited by the available pump power) with a peak power of 0.74 MW for 22 ps pulses with no signs of transverse mode instability. Measurements of the mode content using the S<sup>2</sup> technique showed a negligible level of high order modes (less than 0.3%) in the output radiation even for the maximum output power level. Our reliability tests predict no thermal issues during long-term operation (10<sup>5</sup> hours) of the developed tapered fiber laser up to kilowatt output average power levels.

© 2021 Optical Society of America under the terms of the [OSA Open Access Publishing Agreement](#)

## 1. Introduction

Fiber lasers, in particular ytterbium-doped fiber lasers, have a number of advantages such as high output beam diffraction-limited quality, high optical-to-optical efficiency and simplicity of design. However, the development of an all-fiber system with simultaneously high average power and high peak power while maintaining the diffraction-limited beam quality is quite a challenging task. The main limiting factor for peak power scaling is a relatively low threshold of nonlinear effects such as stimulated Raman scattering (SRS), self-phase modulation and four-wave mixing. The threshold can be increased only by using short-length large mode field area (LMA) fibers. The main drawback of this approach is that the core of most LMA fibers supports a few modes, thus the single mode operation regime is realized via the differential modal gain regime [1], and, in some cases, by the method of selective excitation of the fundamental mode [2]. As a result of the presence of high order modes, the maximum achievable average power level is limited by the onset of thermal effects leading to degradation of the output beam quality due to changes in the waveguide structure (thermally induced refractive index change) or the mode instability effect (a signal power coupling between the fundamental mode and the first high-order mode occurring on a thermal long-period grating induced by mode interference) [3]. In a previous paper [2], a record-high peak power level has been achieved by using a photonic-crystal fiber (PCF) with a core diameter of 108 μm and a length of 1.4 m. The authors were able to amplify 3 ns pulses with up to 1 MW of peak power at the fiber output, but the average power was only 10 W as it was restricted by the onset of amplification of cladding modes at higher levels of

average power. For convenience, the results provided in this section are summarized in Table 1. The same authors demonstrated amplification of 0.8 ns pulses to up to 950 W of average power with only 15 kW of peak power by means of a step-index fiber (SIF) with a significantly smaller core diameter (mode field diameter of 27  $\mu\text{m}$ ) [4]. In [5], the authors demonstrated a SIF with a highly Yb-doped 33  $\mu\text{m}$  low-NA core and Ge-doped cladding and bulky system based on it that is capable of amplifying 190 ps pulses to up to 530 kW of peak power and 150 W of average power. However, an all-fiber system based on a SIF with a 30  $\mu\text{m}$  core diameter was able to generate pulses with 125 W of average power and only 15 kW of peak power at the fiber output [6]. Recently, amplification of 3 ns pulses up to simultaneously high peak power and high average power of 0.9 MW and 130 W (the authors claimed powers of 1 MW and 150 W, but that result was obtained far above the mode instability threshold), correspondingly, has been demonstrated in a bulky system based on a rod fiber with a core diameter of 100  $\mu\text{m}$  [7]. In that case, further average power scaling was limited by the onset of the mode instability. To the best of our knowledge, the latter result is a record high for fiber systems. However, such a system consists of a large number of bulk optics and high precision translators, thus it lacks one of the main advantages of all-fiber systems – maintenance-free operation.

**Table 1. Results for peak and average power demonstrated with different LMA fiber types**

Fiber type	Peak power, kW	Average power, W	System implementation	Reference
Photonic crystal fiber	1000	10	Bulk	[2]
Step index fiber	15	950	Bulk	[4]
Step index fiber	530	150	Bulk	[5]
Step index fiber	15	125	Monolithic	[6]
Rod fiber	900	130	Bulk	[7]
Tapered fiber	110	200	Monolithic	[9]
Tapered fiber	2000	17	Monolithic	[10]
Tapered fiber	700	10	Monolithic	[12]
Tapered fiber	292	28	Monolithic	[11]

One of the promising LMA designs is an active tapered fiber. In such a design, the core and the cladding increase in diameter along the fiber length, with a robust single mode core at the thin end and a core that is several times larger in diameter at the thick end, which, therefore, has a larger mode field diameter. The smooth-enough increase in diameters ensures an adiabatic increase in the fundamental mode area propagating from the thin to the thick end of the fiber, even in the case of transition from 7  $\mu\text{m}$  up to 117  $\mu\text{m}$  [8]. In [9] authors have demonstrated a high-power master oscillator power amplifier (MOPA) with a final stage based on a short-length 2.5 m Yb-doped tapered fiber with a 50  $\mu\text{m}$  core at the output end allowing the achievement of 200 W of average power and 0.11 MW of peak power in 49 ps pulses with a good output beam quality ( $M^2$  was 1.3). Another group of researchers [10] utilized a 0.9-m-long Yb-doped tapered fiber with a 52  $\mu\text{m}$  core to achieve a record-high level of 2 MW of peak power, but with an average power level of only approximately 17 W. In our previous paper [12], we also have demonstrated the possibility of achieving high-peak power (0.7 MW) by means of a tapered fiber, which is comparable with results demonstrated in PCF-based systems. However, the average power level of our system was only 10 W. At the moment, the best result in terms of obtaining high peak and average power simultaneously by utilizing a tapered fiber was obtained in [11] where 28 W of average power and 292 kW of peak power with diffraction limited beam quality ( $M^2 < 1.1$ ) was demonstrated. The main goal of the present paper is to investigate the prospects of tapered fiber design for simultaneous achievement of high peak and average powers in picosecond pulses, while maintaining diffraction-limited beam quality. Also creation of such a system should meet

the industry demand for compact and robust sources of pulsed radiation with simultaneously high peak and average power for high processing speed of materials.

## 2. Experiment

For this work, we realized a series of ytterbium-doped polarization-maintaining (PANDA type) tapered fibers using the non-stationary fiber drawing process [12]. This technique allows us to fabricate series of tens of tapered fibers during one drawing, while keeping main fiber parameters (refractive-index profile shape, core roundness, ability to maintain polarization and etc) unchanged along the tapered fiber length. The core of the fabricated fibers was based on phosphoraluminosilicate photodarkening-free glass matrix doped with 2 wt.% of  $\text{Yb}_2\text{O}_3$ ; the typical fiber had a total length of 2.45 m, with core, first and second cladding diameters of 46  $\mu\text{m}$ , 330  $\mu\text{m}$ , and 410  $\mu\text{m}$ , respectively, at the thick end of the fiber (Fig. 1(a)). The small-signal absorption from the first cladding was measured to be  $\sim 25$  dB/m at a wavelength of 976 nm (Fig. 1(b)). The fiber had an all-glass design (see the fiber cross section photo in the inset of Fig. 1(a)) with numerical aperture (NA) of the first cladding in excess of 0.26, the core NA was  $\sim 0.095$  ( $\text{dn} = 0.003$ ). As it can be seen from Fig. 1(c), we have realized the so-call W-type refractive index profile (depression layer around the core). The input core with diameter of 9.5  $\mu\text{m}$  has  $\text{LP}_{11}$  cut-off wavelength of  $\sim 1000$  nm (obtained by solving wave equation for measured RIP rescaled to 9.5  $\mu\text{m}$  core). The output core with diameter of 46  $\mu\text{m}$  supports 112 modes (including polarization multiplicity).

The standard MOPA scheme was realized by using the tapered fiber in the final amplification stage. The master oscillator was a commercially available generator of 5 ps pulses with a central wavelength of 1064 nm and a variable repetition rate from 0.92 MHz to 18.4 MHz and maximum average power (at 18.4 MHz) of 5 mW obtained from Fianium Ltd. These pulses were preamplified and stretched in a low-power part of the system (two stages based on in-home made 6/125  $\mu\text{m}$  Yb-doped PM fibers in-core pumped via wavelength division multiplexer with radiation from single mode diodes centered at 976 nm and one stage based on in-home made 10/125  $\mu\text{m}$  Yb-doped PM double-cladding fiber, that cladding pumped by 915 nm multimode diode via pump-combiner), and, at the input end of the tapered fiber, we obtained 22 ps pulses with an average power of up to 0.5 W. The seed signal was coupled into the core of the tapered fiber by splicing of the output fiber of the low-power stage of the system to the thin end of the tapered fiber by means of a standard fusion splicer system. The signal output (thick) end of the tapered fiber was mechanically angle-polished to avoid parasitic generation and fixed onto a water-cooled aluminum plate. Pump radiation from three wavelength stabilized multimode diodes manufactured by BWT Ltd. (each diode had a numerical aperture of 0.15, with an output power of 130 W, 100 W and 50 W for the first, second and third diodes, respectively) was summed up into one fiber with a core diameter of 200  $\mu\text{m}$  by means of a 3 to 1 combiner and then coupled into the first cladding of the tapered fiber through its thick end by means of two lenses ( $f=11$  mm) and a dichroic mirror ( $\text{HR}@1064$  nm and  $\text{AR}@976$  nm). See Fig. 2 for the setup scheme. Then, the output radiation from the whole system was characterized by an optical power meter, Ophir, optical spectrum analyzer Yokogawa AQ6370C, autocorrelator Inrad 5-14B,  $M^2$  measurement system from Thorlabs and a fabricated in-house setup for spectral and spatial ( $S^2$ ) image resolution [13]. For the  $S^2$  method, we had to replace the pulsed seed source by a homemade superluminescent source providing continuous-wave radiation with 0.25 W of average power, 15 nm of bandwidth at full width half maximum and a central wavelength of 1064 nm. It should be noted that usage of pulsed source for  $S^2$  method is undesirable as possible phase change due to nonlinear effects results in impossibility to retrieve the phase of mode (important for correct identification of mode type). At the same time, from [14–17] the presence of stimulated Raman scattering effect or Kerr effect (resulted in self-phase modulation effect) in amplifiers based on step-index or graded-index fibers leads at first to output beam

quality improvement (first SRS Stokes generates in the fundamental mode, Kerr effect results in beam self-cleaning). However, that is not the case if pulse peak power is close to self-focusing effect threshold and/or in the presence of central-dip in fiber refractive index profile [10]. In our case, the fiber have nearly perfect step-index profile, in MOPA the SRS will be kept at low level (<1%) and peak power will be considerable lower than self-focusing threshold value, thus  $S^2$  method with continuous-wave source will show the worst possible case for pulsed amplifier.

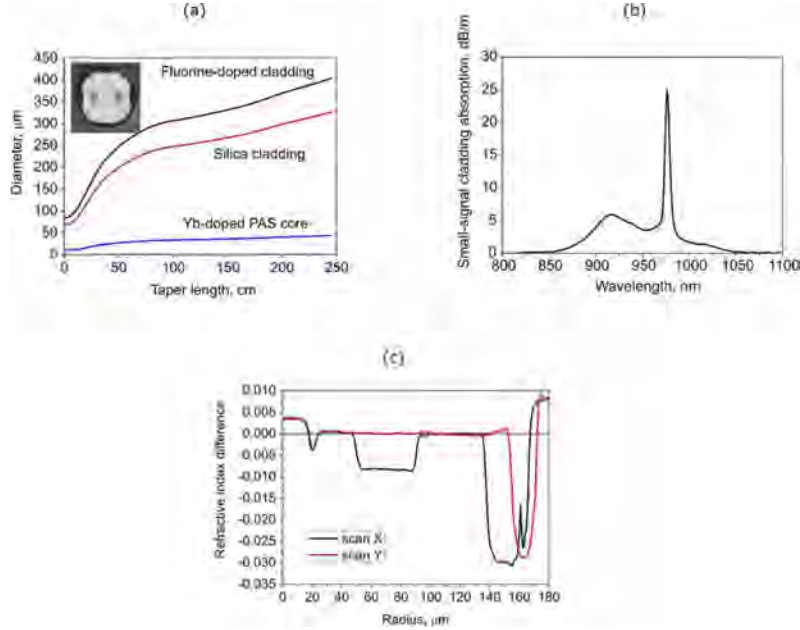


**Fig. 1.** (a) Dependence of the core, first and second cladding diameters on the length of the realized ytterbium-doped tapered fiber. A photograph of the fiber cross section is shown inset. (b) The spectrum for the small-signal absorption from the first silica cladding. (c) Measured refractive index profile of the tapered fiber with second cladding diameter of 340  $\mu\text{m}$ .

### 2.1. Limiting factor for average power scaling

A main factor limiting average power scaling in a tapered fiber is the vignetting effect [18,19]. The vignetting is caused by the fact that the numerical aperture (NA) for radiation that propagates along a tapered fiber from the thick end down to the thin end increases. At some point of a tapered fiber, obviously somewhere at the transition region with a rapid decrease in diameter, the radiation NA will exceed the guiding structure NA and the radiation will leak from the structure. This effect can have a positive impact on the small-signal gain value due to the introduction of high losses for the backward amplified spontaneous emission (ASE) [12]. However, in the case of pump radiation for which the power is orders of magnitude greater than the power of the backward ASE, the leakage of radiation at some point of a tapered fiber can damage it via heating and degradation of the polymer coating. One can use the inequality (1) to estimate the first cladding diameter value at which leakage will occur:

$$D_{\text{first clad}}(z) < \frac{NA_{\text{input}}}{NA_{\text{max}}} D_{\text{first clad}}(L), \quad (1)$$

where  $D_{\text{first clad}}(z)$ ,  $D_{\text{first clad}}(L)$  are the first cladding diameters of a tapered fiber at some position  $z$  along the length of the fiber where leakage occurs and at the thick end of a tapered fiber ( $L$  is

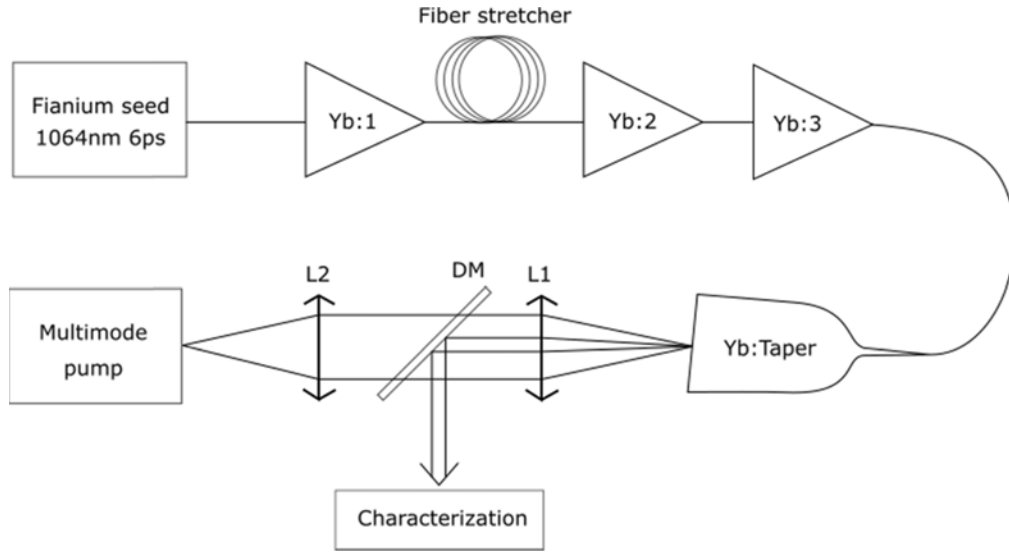


**Fig. 2.** The realized MOPA scheme with the tapered fiber in the final amplification stage. Yb:1, Yb:2 are low-power core-pumped stages, Yb:3 is cladding-pumping stage, DM is dichroic mirror, and L1, L2 are lenses with  $f=11$  mm.

length of the tapered fiber), respectively;  $NA_{input}$ ,  $NA_{max}$  are the numerical apertures for the pump radiation and light guiding structure formed by the first and second cladding of a tapered fiber, respectively.

The value of the vignetting losses can be estimated from Eq. (2):

$$\alpha_{vign}(z) = \frac{20}{\ln 10 \cdot D_{first\ clad}(z)} \cdot \frac{dD_{first\ clad}(z)}{dz}, \quad (2)$$

The temperature of the leakage point is determined by a number of factors, including absorption of the fiber coating polymer and other surrounding materials. However, to define the hottest leakage point, one should take into account the unabsorbed pump power and the diameter of the tapered fiber that determines the surface area through which leakage occurs:

$$T(z) = C \cdot \alpha_{vign}(z) \cdot \frac{P_{pump}(z)}{D_{clad}(z)},$$

where the coefficient  $C$  is determined mainly by the characteristics of the materials surrounding the fiber, the heat removal efficiency and other parameters, but is almost independent of the  $z$  coordinate.

In this work, to minimize heating of the tapered fiber at the leakage point during experiments, in other words – to minimize the  $C$  coefficient, the fiber was fixed onto an aluminum spool with a diameter of 18 cm by double-sided adhesive thermal conductive tape. This construction, on the one hand, provides efficient heat removal from the tapered fiber, and, on the other hand, minimizes the absorption of the pump radiation in the vicinity of the fiber (most of the pump, which is no longer guided by the secondary cladding, passes out of the fiber to the air without heating the polymer coating and aluminum spool).

First, we have conducted an experiment in order to determine the maximum pump power that can be handled by the transition region of the tapered fiber, in other words – the level of pump power at which the leakage point burns as a result of the vignetting effect. The most thermal sensitive component of the fiber is the protective polymer coating – we used standard DeSolite

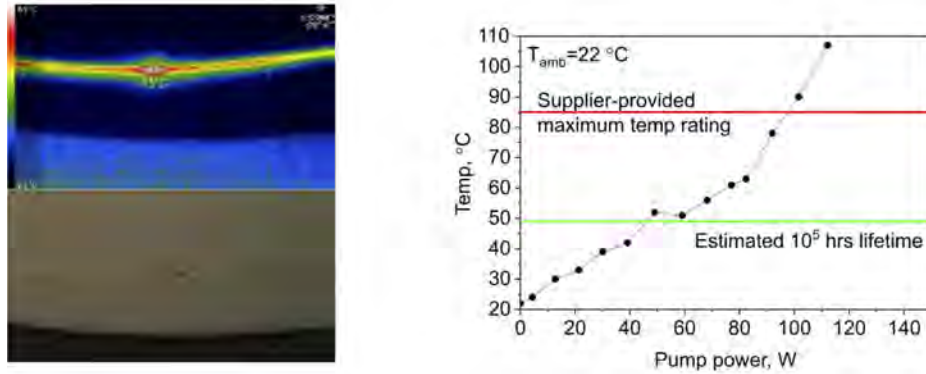
3471-3-14 acrylate that is designed to operate in a temperature range from  $-60^{\circ}\text{C}$  to  $85^{\circ}\text{C}$  [20]. To determine the thermal capabilities of the polymer coating under laser radiation, we have shortened one of the tapered fibers down to 0.8 m in length by cutting-off its thick part, making the absorption of the pump radiation negligible, and, thus, all the pump radiation coupled into the thick end of the fiber reaches the leakage point. By obtaining the dependence of the polymer temperature at the leakage point on the input pump power, we determined a maximum allowable operational temperature. During the experiment, we controlled the temperature of the leakage point by means of a SeekThermal thermal viewer, and the data obtained are depicted in Fig. 3(a). The experiment showed that the polymer burns at a temperature of  $110^{\circ}\text{C}$ , corresponding to a pump power of 110 W. Then, we estimated the temperature of the leakage point at which the polymer will work for 100 000 hours of continuous operation, which corresponds to the lifetime of the best commercially available pump diodes. For this, a series of experiments, similar to the abovementioned experiment, were carried out in which the lifetime (time needed for polymer to start burning) of the polymer at the leakage point of the fiber operating at different temperatures was measured. During experiment we have performed only one measurement for each point (the accuracy on the same order as size of the symbol in Fig. 3(b)). An extrapolation of the data obtained by a decaying exponential function to 100 000 hours gave us a temperature value of  $49^{\circ}\text{C}$  (Fig. 3(b)) that corresponds to approximately 47 W of pump power (Fig. 3(a), right).

It is worth clarifying that in a longer tapered fiber, almost all the pump power will be absorbed in the thick part before reaching the leakage point, thus the maximum possible pump power that can be coupled, and, therefore, the maximum output signal power, will be considerably higher than that in the abovementioned experiment. To estimate the maximum possible pump power level that can be coupled in the realized tapered fibers with different lengths (ranging from 1.35 to 2.45 m), simulation software, written by us, that solves the rate equations by 4<sup>th</sup> order Runge-Kutta method was used. These equations consider the power of the signal, pump, forward and backward amplified spontaneous emission and the leakage point position and losses using Eqs. (1) and (2). In the simulation, we varied the length of the tapered fiber by cutting it from the thick end (not shrinking it); the signal was continuous wave at 50 mW and 1064 nm, the pump was at 976 nm with 0.22NA. As a criterion for the maximum coupled pump power, we used the condition that the unabsorbed pump power at the leakage point should not exceed 47 W, corresponding to a predicted polymer lifetime of 100 000 hours, as defined above. From the simulation data shown in Fig. 4, it can be seen that with increasing length, the maximum coupled pump power value grows almost exponentially up to  $\sim 1.7$  kW (red curve). The predicted output signal power was estimated to be  $\sim 1.4$  kW (Fig. 4, green curve) at a pump power level of  $\sim 1.7$  kW. It should be noted that currently commercially available pump combiners can couple pump from 19 fiber ports (core  $D = 105\text{ }\mu\text{m}$ , clad NA  $\sim 0.15$ , maximum power  $\sim 100$  W) into one  $400\text{ }\mu\text{m}$  core fiber with NA $\sim 0.22$  (can be coupled into our tapered fiber). So up to 1.9 kW of pump power might be coupled to the tapered fiber.

## 2.2. Limiting factor for peak power scaling

It is well known that for a regular fiber with a constant diameter for the core and cladding, an increase in the fiber length results in a decrease in the threshold for nonlinear effects. For this reason, the previously mentioned method of average power scaling for tapered fibers seems to be not optimal in terms of peak power. However, in our previous paper [12], it was shown that the choice of a pump wavelength of 976 nm and a signal wavelength of 1064 nm enables an operational regime in which the nonlinear effects threshold increases with the tapered fiber length. This effect can be explained by comparison of the nonlinear effects threshold (the stimulated Raman scattering (SRS) one) in a tapered fiber and a regular fiber with similar core and cladding diameters at the output end ( $40\text{ }\mu\text{m}$  core and  $320\text{ }\mu\text{m}$  cladding, input end of the tapered fiber was  $10/80\text{ }\mu\text{m}$ ) and the same pump power absorption coefficient (cladding absorption of 25 dB/m at

(a)



(b)

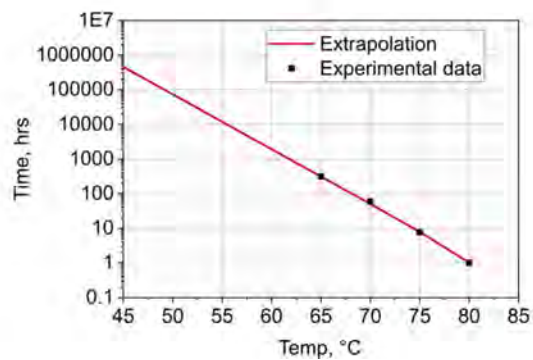


**Fig. 3.** The experimental data for the thermal capabilities of the DeSolite polymer: (a) top left – a thermal viewer photo of the leakage point, bottom left – a photo of the leakage point after polymer burning, right - the dependence of temperature at the leakage point on input pump power and (b) lifetime of the DeSolite polymer for different temperatures at the leakage point.

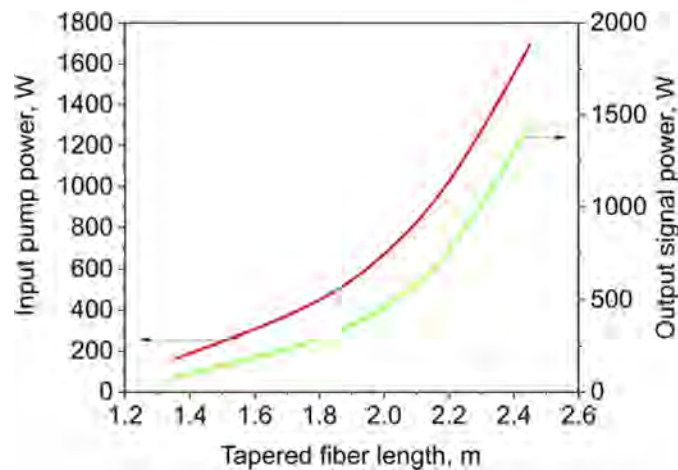


**Fig. 4.** Estimation of the maximum coupled pump power and the achieved average output power for an amplifier based on a realized tapered fiber with different lengths.

976 nm). These fibers were investigated using the abovementioned amplifier simulation software; for the simulations, the seed signal had an average power of 1 W, which is high-enough to saturate both the fibers (tapered and regular), the repetition rate was 10 MHz and the pulse duration was 8 ps. We calculated the SRS threshold by directly solving the rate equations, which included a seed due to vacuum fluctuations (one photon per unit frequency per unit time per mode) [21] at the first Stokes wavelength (1125 nm for 1064 nm signal) and ASE, generated in the amplifier at this wavelength. The threshold was set at the amplification of the SRS signal at the first Stokes wavelength to more than 1% of the main signal.

Three cases were considered: a regular fiber with a copropagating pump power, a regular fiber with a counterpropagating pump power and a tapered fiber with a counterpropagating pump power (0.5 m from the beginning of the fiber was a linear taper and rest of the fiber have constant core and cladding diameter). The estimated dependence of the SRS threshold (the output signal peak power at which 1% of the power is contained in the first Stokes component of SRS is referred to as the SRS threshold) on the fiber length for all the cases is depicted in Fig. 5(a). As shown in this figure, the SRS threshold for the copumped regular fiber exhibits an inverse dependence on the fiber length, as expected. For the case of a counterpumped regular fiber, the situation is different: the SRS threshold decreases until the fiber length reaches 1 m value, which is high enough to absorb all the pump power, and then the threshold value almost stands still with a tendency to increase slightly. This behavior is easily explained by the fact that the considerably long fiber is able to absorb all the coupled pump power in the pump input part, while the other side of the fiber remains unpumped and no growth of signal takes place in this part, thus signal amplification occurs in the last ~1 m of the fiber near the pump input end. In the case of the tapered fiber, the situation is similar with the exception that the signal input end of the fiber has a small-diameter core. Therefore, high amplification at this part results in a quick onset for nonlinear effects. The increase in the length of the tapered fiber suppresses the evolution of the nonlinear effects in the thin part of the fiber and enables achievement of the SRS threshold value demonstrated by the counterpumped regular fiber, which is numerically forced to operate in the single mode regime. Therefore, the choice of a long-length tapered fiber allows one to achieve a nonlinear effect threshold that is close to the threshold achievable in a regular fiber with the same core and cladding diameters. Note that we do not consider the shortest tapered fiber (to achieve the highest SRS threshold value), as in this case a huge amount of unabsorbed pump radiation will reach the leakage point and damage fiber.

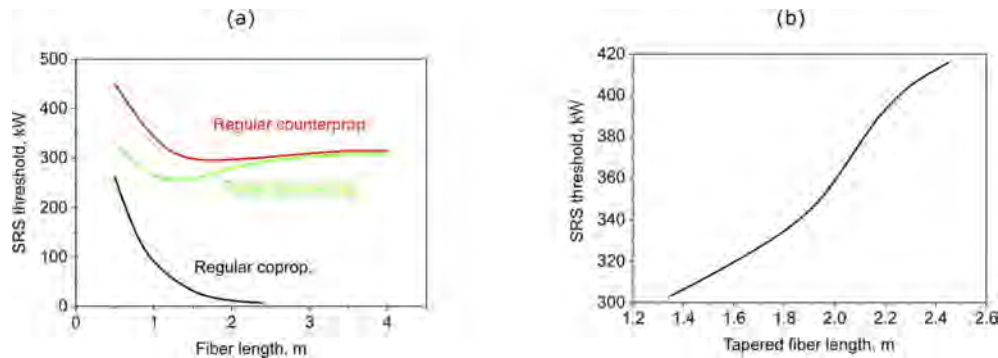


**Fig. 5.** Estimate of the dependence of the SRS threshold on fiber length for (a) model tapered and regular fibers under different pump conditions and (b) a realized tapered fiber.

Note that the regular fiber always demonstrates a higher SRS threshold compared to the tapered fiber (only for a long fiber length this threshold is nearly the same), but, in a real experiment, it is quite challenging task to achieve single mode operation in a regular fiber with a 40  $\mu\text{m}$  core – this is why we need a tapered fiber to realize both diffraction-limited beam quality and a very high threshold for nonlinear effects. A necessary condition for achieving such an amplification regime is the 1064 nm signal wavelength for which the first Stokes component of the SRS is out of the ytterbium ion amplification band. The theoretical dependence of the SRS threshold for the realized tapered fiber on fiber length is shown in Fig. 5(b) (in this case, for simulations the seed was 0.05 W of average power, 8 ps pulse duration and repetition rate of 10 MHz). On Figs. 5(a) and (b) tapered fiber have different trends in the SRS threshold grow because it have a different diameter profile along the length and different seed source was considered in simulations.

### 2.3. Final experiment

A final series of experiments were conducted to test the theoretically obtained results. We do not have access to few-kW pump power sources, but available pump sources with a total power of 260 W (after 3-to-1 pump combiner and collimating lens L2 – see Fig. 2) allow us to verify whether or not the tapered fibers can surpass the record-high result of a 130 W average power and 0.9 MW peak power demonstrated with rod-type fiber in [7]. The experimental setup used is the same as that depicted in Fig. 2. In these experiments the tapered fiber from Fig. 1 was used in the final high-power stage. The maximum fiber length was chosen to be  $\sim 2.45$  m – at larger tapered fiber length no noticeable increase of SRS was observed in Fig. 5(a).

In the first series of experiments, we investigated the operation of a tapered fiber amplifier that was seeded with 22 ps pulses with an average power of 0.5 W (which is a quite-high power level to ensure safe operation of an amplifier providing a high value for the signal gain) and a repetition rate of 18.4 MHz. These pulses were amplified with a differential efficiency of 72% in the tapered fiber up to an average power of 144 W (here and further for power calculation we determined percentage of spectral power in the signal band) corresponding to a peak power of 350 kW assuming a Gaussian pulse shape (see Fig. 6(c) for ACF, multi-pulse trace is showed in inset on Fig. 6(c)). The first Stokes peak from SRS was considerable, but its absolute value was only 1%. The temperature of the polymer of the tapered fiber (especially its transition region) was monitored during experiments, and even at highest level of average power it was at ambient temperature level of 22  $^{\circ}\text{C}$ .

We have also measured the polarization extinction ratio (PER) of the signal at the tapered fiber output using a Glan-Taylor prism, and the PER value was found to periodically vary from 13.5 dB to 14.5 dB along the full operational range, that is typical for active tapered fibers

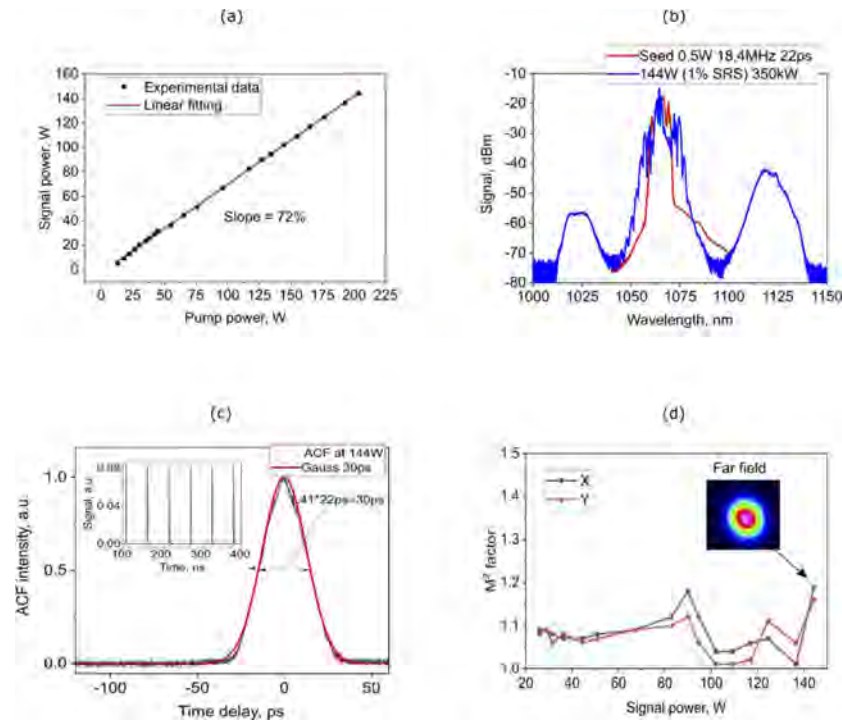


**Fig. 6.** The experimental results obtained for a seed with an average power of 0.5 W and a repetition rate of 18.4 MHz: (a) differential efficiency, (b) spectrum of the seed before the tapered fiber and at an average power of 144 W at the tapered fiber output, (c) autocorrelation function of the pulses at an average power of 144 W and its Gaussian fitting and multi-pulse trace in the inset, (d)  $M^2$  factor measurements and output beam intensity distribution at far field at 144 W in inset.

[9,22]. Polarization extinction properties of tapered fibers produced during drawing process, are discussed in details in [23], thus we do not discuss it here. But we want to notice that tapering during fiber drawing process used in our work means that «temperature impact» on every point along the fiber is absolutely the same, thus geometry of thick and thin parts of the fiber should not (and we believe, could not) vary significantly. In this aspect tapered fiber produced by drawing have advantage over post-produced tapers [10], where tapered part fabricated in a separate process from end of regular fiber using special equipment (for example, Vytran glass processing station) and affected by additional heating, while thick regular part is not affected at all. As a result, in post-produced tapered fibers the cross section geometry and refractive index profile might vary significantly along the length of fiber, that might result in output mode shape quality degradation and in deterioration of polarization extinction ratio.

The tapered fiber beam quality was studied by a conventional  $M^2$  factor measuring method and the mode content was studied by the  $S^2$  technique [13]. The  $M^2$  factor during the above experiment was measured to be approximately 1.1 over the whole range of the output signal power from 25 W to 144 W (Fig. 6(d)), exhibiting some fluctuations after a power level of 100 W. These fluctuations were caused by imperfections in the experimental techniques used: we paid little attention to thermal management of the pump coupling unit, while the path from output end of the tapered fiber to  $M^2$  system was quite long; these factors led to slight displacement of beam on the CCD camera of  $M^2$  system, resulted in a slight variation of the measured  $M^2$  factor.

Then, we investigated the exact mode content of the tapered fiber amplifier at a high level of output signal by using the  $S^2$  technique. This consisted of point-by-point scanning of the output beam using a single mode fiber coupled into an optical spectrum analyzer. These spectra were mathematically treated to reveal the mode content at the beam. For this, we had to replace the pulsed seed source with a CW superluminescent source, as described in the beginning of the section. As shown in Fig. 7, the multipath interference (MPI) graph at 150 W of output power exhibits a few peaks, but the only meaningful peak is the one with a delay of 0.705 ps with a -25.7 dB MPI corresponding to the  $LP_{11}$  mode (see retrieved mode intensity and phase shown in the inset, which correspond to the intensity and phase of the  $LP_{11}$  mode). The output intensity in the inset at Fig. 7 is for output beam at far field obtained by  $S^2$  set-up and color of each point of the image corresponding to optical power coupled into single mode fiber that used for point-by-point beam scanning. Some distortion of the output intensity shape and phase retrieved for the  $LP_{11}$  mode was caused by slight movements of output end of the tapered fiber, that was unavoidable at average power level in excess of 100 W, and very long-term measurements (about 30 minutes). Obtained data shows that the high order mode content in the output radiation of the tapered fiber amplifier is quite low (less than 0.3%) and no transverse mode instability is observed up to 150 W of average power (limited by available pump power), which is the record for average power of sub-MW-peak-power diffraction-limited-beam-quality pulse fiber lasers. It should be noted that a much higher average power of 379 W was achieved in continuous wave regime using a short tapered fiber ( $\sim 1.3$  m in length) by Lai et. al. [22], thus we expect that farther power scaling without deterioration of the output beam quality is possible in our amplifier when more powerful pump diodes are used.

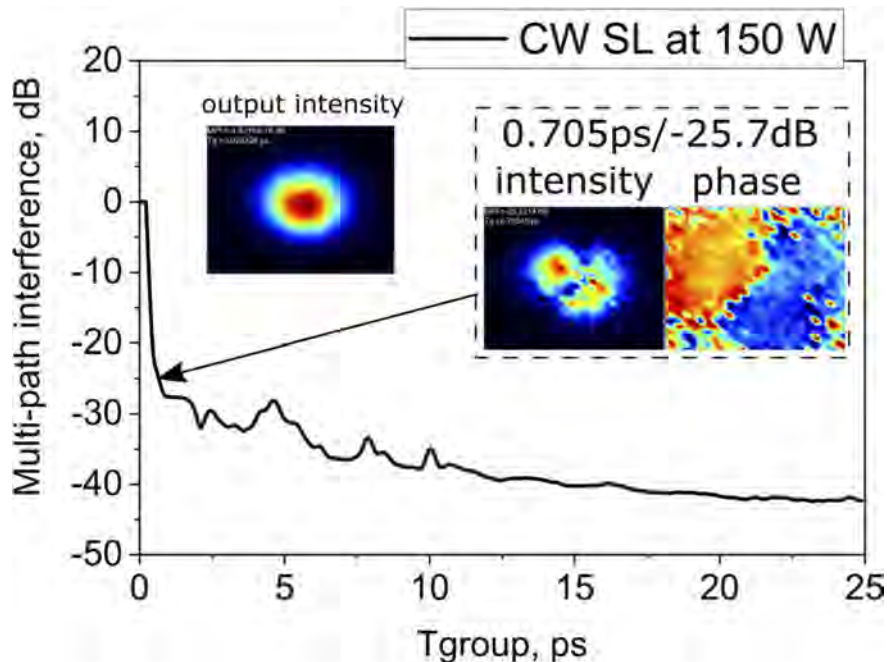


**Fig. 7.** Investigation of the tapered fiber amplified mode content by the  $S^2$  technique at an output power of 150 W.

Next, we conducted experiments for the amplification of a weaker seed signal in order to achieve a higher level of peak power. In our previous paper [12], we showed that tapered fibers require an average power for a seed that is a few magnitudes lower in comparison to regular fibers.

For the experiments, we decreased the average power of the seed down to 10 mW and decreased the repetition rate down to 9.2 MHz. This allowed us to achieve a peak power level of 740 kW at 150 W of average power assuming a Gaussian pulse shape (see Figs. 8(a)-(c)). The SRS threshold value is almost twice higher than that for theoretically demonstrated on Fig. 5(b), because the seed at the taper input had average power of two orders lower (0.01 W against 1 W). Lowering the seed signal average power resulted in an extremely low level of SRS (0.03% from spectrum) but also in a higher level of amplified spontaneous emission (1.3% from spectrum). The beam quality of the system output radiation was good:  $M^2$  of 1.14/1.03 at 150 W (see Fig. 8(d)). At 150 W of average power, the temperature of the polymer at the transition region of the tapered fiber was measured to be at ambient temperature level of 22 °C. Further decrease in repetition rate in order to increase peak power does not affect SRS threshold, but led to considerable lower average output power.

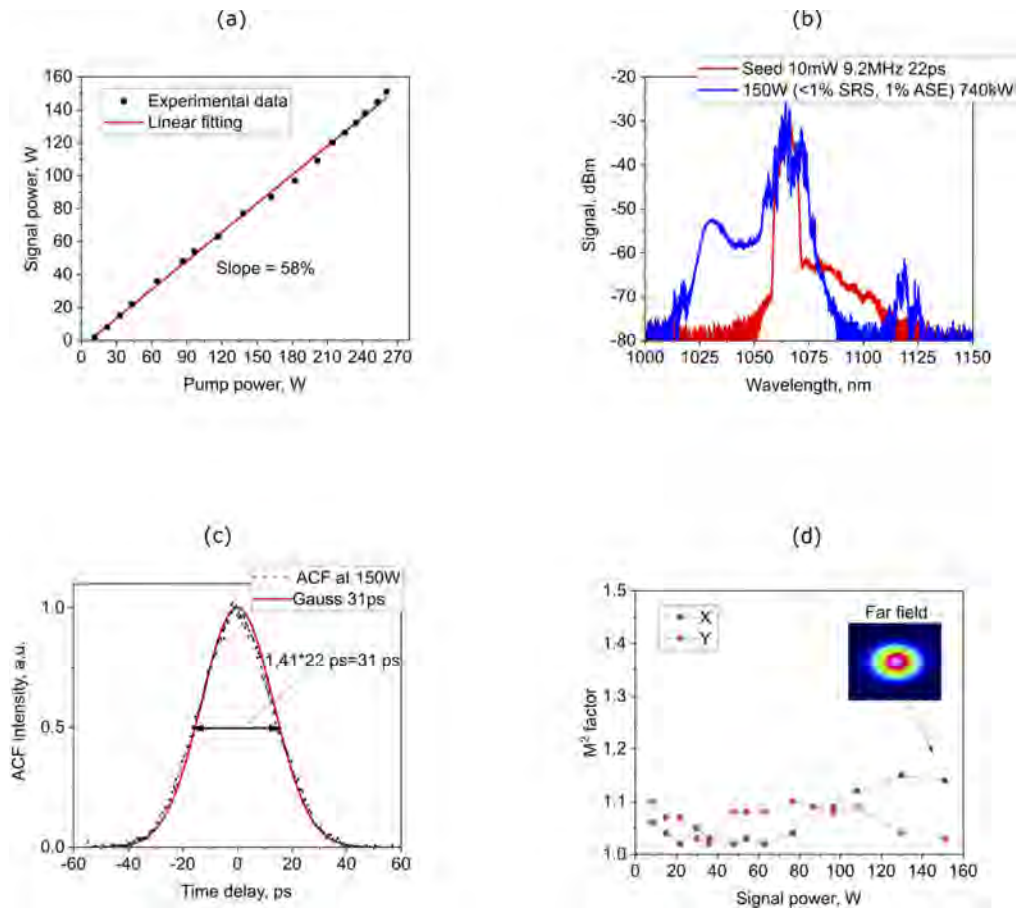


**Fig. 8.** The experimental results obtained for a seed with an average power of 10 mW and a repetition rate of 9.2 MHz: (a) differential efficiency, (b) spectrum of the seed before the tapered fiber and at an average power of 150 W at the tapered fiber output, (c) autocorrelation function for the pulses at an average power of 150 W and its Gaussian fitting and multi-pulse trace in inset, (d)  $M^2$  factor measurements and radiation intensity distribution at far field for 150 W.

### 3. Conclusion

In this paper, we demonstrated promising prospects for a tapered fiber design for picosecond pulse amplification up to simultaneously high peak and high average powers. An average power of 150 W and a peak power of 0.74 MW for 22 ps pulses with no signs of transverse mode instability was achieved, which is, to the best of our knowledge, a record for an all-fiber system. A further increase in the signal power was limited only by the available pump power.

**Funding.** Russian Science Foundation (18-19-00687); Conseil Régional de Nouvelle Aquitaine (FLOWA, SCIR, SIP2).

**Disclosures.** The authors declare no conflicts of interest.

### References

1. D. A. Gaponov, S. Février, M. Devautour, P. Roy, M. E. Likhachev, S. S. Aleshkina, M. Y. Salganskii, M. V. Yashkov, and A. N. Guryanov, "Management of the high-order mode content in large (40  $\mu\text{m}$ ) core photonic bandgap Bragg fiber laser," *Opt. Lett.* **35**(13), 2233–2235 (2010).
2. T. Eidam, J. Rothhardt, F. Stutzki, F. Jansen, S. Hadrich, H. Carstens, C. Jauregui, J. Limpert, and A. Tünnermann, "Fiber chirped-pulse amplification system emitting 3.8 GW peak power," *Opt. Express* **19**(1), 255–260 (2011).
3. T. Eidam, C. Wirth, C. Jauregui, F. Stutzki, F. Jansen, H.-J. Otto, O. Schmidt, T. Schreiber, J. Limpert, and A. Tünnermann, "Experimental observations of the threshold-like onset of mode instabilities in high power fiber amplifiers," *Opt. Express* **19**(14), 13218–13224 (2011).
4. T. Eidam, S. Hanf, E. Seise, T. V. Andersen, T. Gabler, C. Wirth, T. Schreiber, J. Limpert, and A. Tünnermann, "Femtosecond fiber CPA system emitting 830 W average output power," *Opt. Lett.* **35**(2), 94–96 (2010).
5. R. Sidharthan, D. Lin, K. J. Lim, H. Li, S. H. Lim, C. J. Chang, Y. M. Seng, S. L. Chua, Y. Jung, D. J. Richardson, and S. Yoo, "Ultra-low NA step-index large mode area Yb-doped fiber with a germanium doped cladding for high power pulse amplification," *Opt. Lett.* **45**(14), 3828–3831 (2020).
6. R. Sun, D. Jin, F. Tan, S. Wei, C. Hong, J. Xu, J. Liu, and P. Wang, "High-power all-fiber femtosecond chirped pulse amplification based on dispersive wave and chirped-volume Bragg grating," *Opt. Express* **24**(20), 22806–22812 (2016).
7. Z. Zhao, B. M. Dunham, and F. W. Wise, "Generation of 150 W average and 1 MW peak power picosecond pulses from a rod-type fiber master oscillator power amplifier," *J. Opt. Soc. Am. B* **31**(1), 33–37 (2014).
8. J. Kerttula, V. Filippov, V. Ustimchik, Y. Chamorovskiy, and O. G. Okhotnikov, "Mode evolution in long tapered fibers with high tapering ratio," *Opt. Express* **20**(23), 25461–25470 (2012).
9. A. Petrov, M. Odnoblyudov, R. Gumenyuk, L. Minyonok, A. Chumachenko, and V. Filippov, "Picosecond Yb-doped tapered fiber laser system with 1.26 MW peak power and 200 W average power output power," *Sci. Rep.* **10**(1), 17781 (2020).
10. M. Leich, A. Kalide, T. Eschrich, M. Lorenz, A. Lorenz, K. Wondraczek, D. Schönfeld, A. Langner, G. Schötz, and M. Jäger, "2 MW peak power generation in fluorine co-doped Yb fiber prepared by powder-sinter technology," *Opt. Lett.* **45**(16), 4404–4407 (2020).
11. A. Fedotov, T. Noronen, R. Gumenyuk, V. Ustimchik, Y. Chamorovskii, K. Golant, M. Odnoblyudov, J. Rissanen, T. Niemi, and V. Filippov, "Ultra-large core birefringent Yb-doped tapered double clad fiber high power amplifiers," *Opt. Express* **26**(6), 6581–6592 (2018).
12. K. Bobkov, A. Andrianov, M. Koptev, S. Muravyev, A. Levchenko, V. Velmskin, S. Aleshkina, S. Semjonov, D. Lipatov, A. Guryanov, A. Kim, and M. Likhachev, "Sub-MW peak power diffraction-limited chirped-pulse monolithic Yb-doped tapered fiber amplifier," *Opt. Express* **25**(22), 26958–26972 (2017).
13. J. W. Nicholson, A. D. Yablon, S. Ramachandran, and S. Ghalimi, "Spatially and spectrally resolved imaging of modal content in large-mode-area fibers," *Opt. Express* **16**(10), 7233–7243 (2008).
14. E. A. Zlobina, S. I. Kablukov, A. A. Wolf, A. V. Dostovalov, and S. A. Babin, "Nearly single-mode Raman lasing at 954 nm in a graded-index fiber directly pumped by a multimode laser diode," *Opt. Lett.* **42**(1), 9–12 (2017).
15. K. Krupa, A. Tonello, B. M. Shalaby, M. Fabert, M. G. Barthélémy, S. Wabnitz, and V. Couderc, "Spatial beam self-cleaning in multimode fibers," *Nat. Photonics* **11**(4), 237–241 (2017).
16. M. S. Astapovich, A. V. Gladyshev, M. M. Khudyakov, A. F. Kosolapov, M. E. Likhachev, and I. A. Bufetov, "Watt-Level Nanosecond 4.42- $\mu\text{m}$  Raman Laser Based on Silica Fiber," *IEEE Photonics Technol. Lett.* **31**(1), 78–81 (2019).
17. H. Delahaye, G. Granger, D. Gaponov, L. Lavoute, S. Aleshkina, M. Salganskii, A. Hideur, M. Likhachev, and S. Février, "Megawatt solitons generated above 2000nm in Bragg fibers," *Opt. Lett.* **44**(11), 2713–2715 (2019).
18. V. B. Veinberg and D. K. Sattarov, [Waveguide Optics], Mashinostroenie, Leningrad, Chap. 5 (in Russian) (1977).
19. V. Filippov, J. Kerttula, Y. Chamorovskii, K. Golant, and O. G. Okhotnikov, "Highly efficient 750 W tapered double-clad ytterbium fiber laser," *Opt. Express* **18**(12), 12499–12512 (2010).
20. [https://www.dsm.com/markets/paint/en/markets-and-applications/telecoms.html#par\\_container](https://www.dsm.com/markets/paint/en/markets-and-applications/telecoms.html#par_container)
21. C. Jauregui, J. Limpert, and A. Tünnermann, "Derivation of Raman threshold formulas for CW double-clad fiber amplifiers," *Opt. Express* **17**(10), 8476–8490 (2009).

22. W. Lai, P. Ma, W. Liu, L. Huang, C. Li, Y. Ma, and P. Zhou, “550 W single frequency fiber amplifiers emitting at 1030 nm based on a tapered Yb-doped fiber,” *Opt. Express* **28**(14), 20908–20919 (2020).
23. V. E. Ustimchik, J. Rissanen, S. M. Popov, Y. K. Chamorovskii, and S. A. Nikitov, “Anisotropic tapered polarization-maintaining large mode area optical fibers,” *Opt. Express* **25**(9), 10693–10703 (2017).